Space Science Reviews (2022) 218:57
https://doi.org/10.1007/s11214-022-00905-3

The Psyche Gravity Investigation

Maria T. Zuber[1] Ryan S. Park[2] Linda T. Elkins-Tanton[3] J.F. Bell III[3] Kristoffer N. Bruvold[2] David Bercovici[4] Bruce G. Bills[2] Richard P. Binzel[1] R. Jaumann[5] Simone Marchi[6] Carol A. Raymond[2] T. Roatsch[5] Charles C. Wang[2] Benjamin P. Weiss[1] Daniel Wenkert[2] Mark A. Wieczorek[7]

Received: 31 May 2021 / Accepted: 5 May 2022 / Published online: 18 October 2022

Abstract

The objective of the NASA Psyche mission gravity science investigation is to map the mass distribution within asteroid (16) Psyche to elucidate interior structure and to resolve the question of whether this metal-rich asteroid represents a remnant metal core or whether it is a primordial body that never melted. Measurements of gravity will be obtained via the X-band telecommunication system on the Psyche spacecraft, collected from progressively lower mapping altitudes. Orbital gravity will allow an estimate of GM to better than 0.001 $km^3\ s^{-2}$. A spherical harmonic model of gravity to degree and order 10 will be achievable and, in concert with spherical harmonic data sets from topography and magnetometry, as well as surface composition data, will provide information regarding the spatial and radial distribution of mass that will be used to constrain the origin and evolution of (16) Psyche.

Keywords Gravity · Asteroid · Remote sensing · Spacecraft

1 Introduction

Critical to achieving the scientific objectives of NASA's Psyche mission is characterization of the asteroid's internal structure. Gravitational mapping of (16) Psyche will add to the

The NASA Psyche Mission: Science Instruments and Investigations
Edited by James F. Bell III, Carol Polanskey and Lindy Elkins-Tanton

M.T. Zuber

1 Department of Earth, Atmospheric and Planetary Sciences, Massachusetts Institute of Technology, Cambridge, MA 02139-4307, USA

2 Jet Propulsion Laboratory, Pasadena, CA 91109, USA

3 School of Earth and Space Exploration, Arizona State University, Tempe, AZ 86387-2001, USA

4 Department of Earth and Planetary Sciences, Yale University, New Haven, CT 06520, USA

5 Institute of Geological Sciences, Free University of Berlin, 12249 Berlin, Germany

6 Southwest Research Institute, Boulder, CO 80302, USA

7 Observatoire de la Côte d'Azur, CNRS, Laboratoire Lagrange, Université Côte d'Azur, Nice, France

quantitative hypothesis testing as to whether the asteroid represents an iron core, a fundamental building block of terrestrial planets (Elkins-Tanton 2016; Elkins-Tanton et al. 2022), or if it consists of unmelted metal-rich material. Gravity will also contribute towards interpretation of spatially large structural features of the asteroid, and provide linkage between surface and subsurface processes. Secondarily, the gravity investigation, in coordination with topography (Jaumann et al. 2022), improves global positioning and the reference frame, increasing the ease of integration of all the Psyche mission data sets.

2 Tracking the Psyche Orbiter

The Psyche spacecraft (Hart et al. 2018) contains an X-band telecom system that provides uplink (7.2 GHz) and downlink (8.4 GHz) radio signal and is used to track the spacecraft via range rate and range observations. Spacecraft Psyche's telecom system features a 2-m diameter high-gain antenna and three low-gain antennae, and radio tracking is accomplished using NASA's Deep Space Network (DSN) using 34-m and 70-m antennae at Goldstone, California, Madrid, Spain and Canberra, Australia. The Psyche spacecraft (Brown et al. 2021) also includes an experimental Deep Space Optical Communications (DSOC) laser communication link that will downlink to the Palomar Observatory.

The Doppler shift of the radio signal detected on Earth is sensitive to the changes in the motion of a spacecraft due to gravitational variations, which can be used to recover the gravity field of the body being orbited. The accuracy is defined by the X-band telecom system performance that is typically of order 0.1 mm s^{-1} at 60-s integration time. Radiometric Doppler tracking occurs as two-way, with the same transmit and receive stations, and sometimes three-way, with a different receiver station.

The Psyche mapping plan (Polanskey et al. 2018) is operationally similar to that of the Dawn mission (Russell et al. 2007; Park et al. 2016), on which a number of members of the Psyche Gravity Team participated, providing important experience. Specifically, the mapping operations plan consists of an approach phase and progression to lower altitude orbits as knowledge of the asteroid's gravity field progressively improves (see Fig. 1). During Orbit C, which is the prime for gravity science, radio tracking data will be acquired regularly over the 100-day orbit phase for a total of at least 35 days (i.e., $\geq$35%), which is expected to be sufficient for a global sampling of Psyche's gravity field. Gravity observations will also be acquired in the lower-altitude Orbit D, during which time measurements of surface composition are prioritized.

Figure 2 shows the latest shape of Psyche (Shepard et al. 2021) from different viewing geometries. The shape, developed using a wide range of observations (Arecibo, ALMA, Keck, VLT, stellar occultation), is used in mission planning. Psyche's mean radius is $\sim$113 km, and compared to previously orbited asteroids and dwarf planets, Psyche is smaller than 1 Ceres ($\sim$470 km) and 4 Vesta ($\sim$265 km), but much larger than 433 Eros (8 km), 26143 Itokawa ($<$1 km), 162173 Ryugu ($<$1 km), and 101955 Bennu ($<$1 km).

DSN range measurements to the Psyche spacecraft, which have an accuracy of 1-2 m, are included in inversions for the gravitational field and associated parameters, though experience dictates that this data type does not add particular strength in the determination of the gravity field. However, even if observations are infrequent ($\sim$1 hour over several days), ranging is valuable in improving (16) Psyche's heliocentric orbital ephemeris (cf. Konopliv et al. 2018).

Corrections for Earth media fluctuations are applied to Doppler and range data at each DSN site. These include daily wet and dry terrestrial troposphere corrections and terrestrial

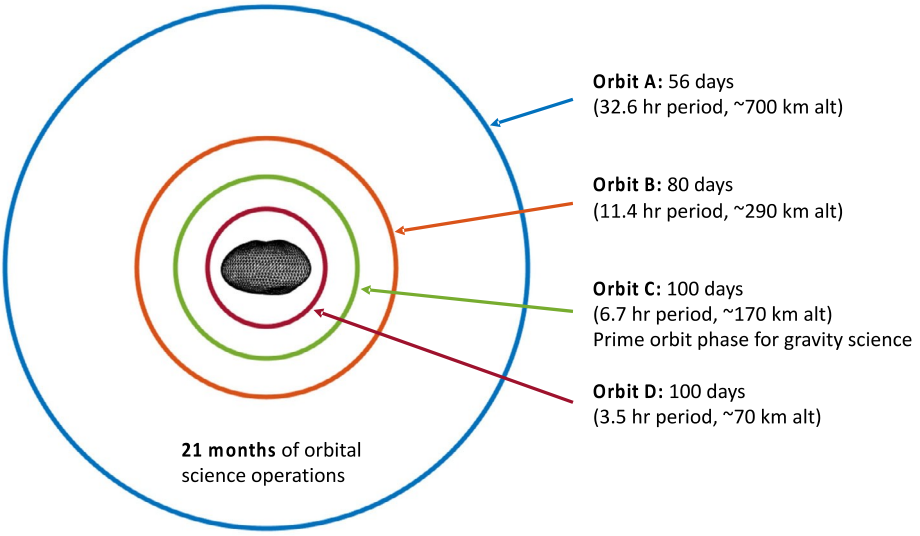

Fig. 1 Schematic depicting the progressive lowering of science mapping orbits, designed based on experience with the Dawn mission. Gravity science is prioritized in Orbit C

GPS-based ionosphere calibrations. The three-way Doppler data are corrected for tracking station timing errors to a level <0.1 mm s^{-1} at 60-s integration time. The range measurements are corrected for spacecraft clock delay and a range calibration correction of <10 m is made at each DSN site (Asmar et al. 2005).

Solar plasma represents an additional source of data noise, with X-band undergoing considerable degradation at Sun-Earth-Psyche (SEP) angles $<20^\circ$, close to solar conjunction (Asmar et al. 2005). Such observations are typically de-weighted in gravity field solutions (see Sect. 3.3). During the entire science mapping phase, the SEP angle will vary essentially from 0° to 180°, so there will be some periods in which tracking is interrupted. However, mission design simulation (Oh et al. 2019) indicates that enough data will be collected during Orbit C with SEP $>40^\circ$ that achieving an $n=10$ gravity field should not be a problem (cf. Fig. 5).

Finally, correction for non-gravitational forces, including angular momentum desaturations and solar radiation pressure modeling of the Psyche spacecraft, is essential. The angular momentum desaturations, often known as small forces, are required to unload large cyclic gravity gradient torques. For Psyche, there may even be non-trivial differences in the gravity gradient torques between a point-mass model and a model with high degree harmonics. During science orbits, environmental torques are compounded much more rapidly when the spacecraft bus is pointing off nadir. Perturbations by small forces are typically a few minutes in duration and will be modeled in 60-s increments. The Psyche spacecraft solar panels will be pointed mostly toward the sun, making the solar radiation pressure fairly smooth and easy to model. However, the spacecraft bus will be rotating relative to the sun to point the instrument deck towards (16) Psyche. The orientation of both the spacecraft bus and panels will be modeled using the attitude of the Psyche spacecraft derived from onboard star trackers and the acceleration due to solar radiation pressure can be typically modeled with accuracy better than 10^{-12} km s^{-2}.

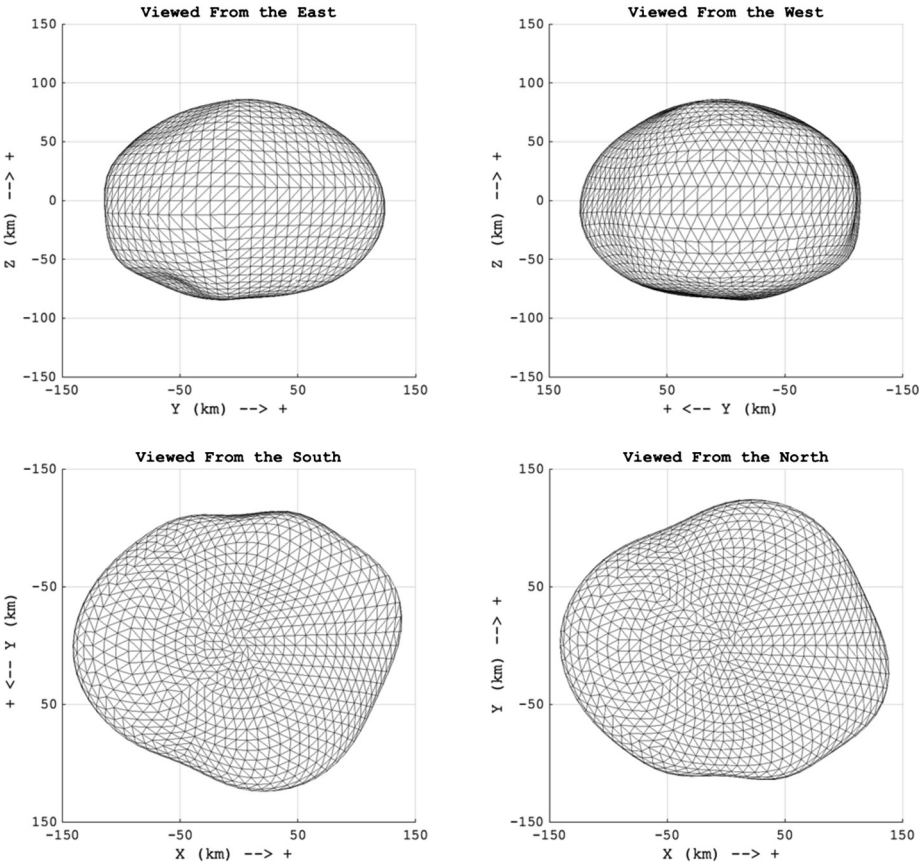

Fig. 2 Shape of Psyche (Shepard et al. 2021) shown from different viewing angles

2.1 Psyche Telecommunication Subsystem

The Psyche Telecom Subsystem operates at X-band for nominal two-way communications (command uplink and telemetry downlink) and two-way tracking (Doppler and ranging). These are the high-level functions, with the details explained in the following sections. The Telecom subsystem block diagram is presented in Fig. 3. This subsystem is block redundant, consisting of two Small Deep Space Transponders (SDSTs), two traveling-wave tube amplifiers (TWTAs), two diplexer-isolators (DXIs), seven waveguide transfer switches (WTS), one high-gain antenna (HGA), and three low-gain antennas (LGAs). Right-hand circular polarization (RHCP) is used for all antennas for nominal operations. Figure 3 also shows how the SDSTs, TWTAs, diplexers-isolators, and two of the waveguide switches (WTS-1 and WTS-2) form a primary and a redundant telecom block. Only one block will be powered on at any given time in flight for nominal operations. Waveguide transfer switches (WTS-3 and WTS-4) are used to route the signals between the antennas and the two telecom blocks. WTS-5, WTS-6, and WTS-7 are used to provide redundant paths to the mission-critical antennas using left-hand circular polarization (LHCP) in case WTS-3 or WTS-4 fails. These three switches will only be actuated in case of a switch failure. The waveguide runs to the mission critical antennas, HGA, +X-LGA, and –Z-LGA, are shown in red in Fig. 3.

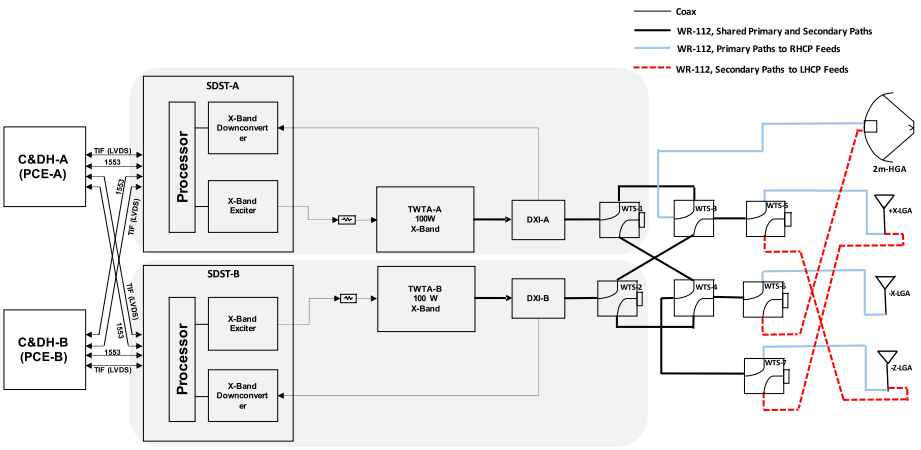

Fig. 3 Block diagram of the Psyche telecommunication system

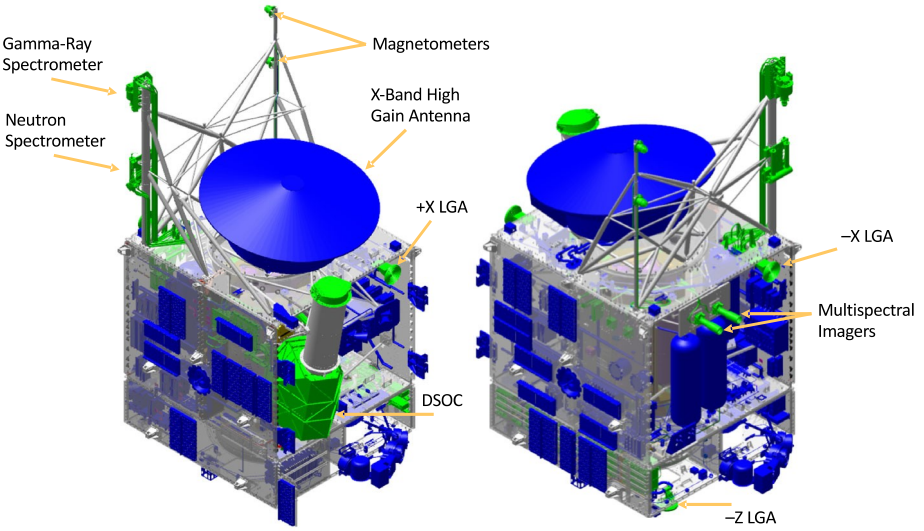

Fig. 4 Schematics showing key components of the Psyche telecommunication system

The locations of the HGA and the three identical LGAs are shown in Fig. 4. The HGA is mounted on the +Z deck of the spacecraft. It supports high-data rate communications, as well as Delta-Differential One-way Ranging (-DOR), and Doppler measurements. In practice, -DOR measurements will be acquired during cruise, but probably not during the orbital phase as Doppler data are much more sensitive. The -Z-LGA, +X-LGA, and -X-LGA are mounted at the -Z, +X, and -X decks of the spacecraft, respectively. The -Z-LGA will provide most of the two-way Doppler measurements for gravity science. It is also used for safe mode communication during the early part of the mission. The +X-LGA is used for safe mode communication for most of the mission. In safe mode, the spacecraft will point the +X-axis of the spacecraft to the sun to charge the solar arrays to ensure the

Table 1 Psyche GM Values

Source	Value $\pm \sigma$ ($km^3 s^{-2}$)
Viateau et al. (2000)	1.15 ± 0.35
Kuzmanoski et al. (2002)	4.49 ± 0.37
Kochetova (2004)	1.78 ± 0.29
Baer et al. (2008)	1.71 ± 0.23
Somenzi et al. (2010)	3.06 ± 1.29
Baer et al. (2011)[a]	1.51 ± 0.06
Konopliv et al. (2011)	1.65 ± 0.46
Carry (2012)	1.82 ± 0.50
Kuchynka et al. (2013)	1.18 ± 0.28
Baer and Chelsey (2017)	1.53 ± 0.05
Siltala and Granvik (2021)	1.12 ± 0.20

[a]The study of Baer et al. (2011) is considered to be the best determination and is used for mission planning purposes

spacecraft is power-positive, with the Earth staying within 40 ° of the +X-LGA boresight. Both +X-LGA and -X-LGA are used to support two-way Doppler measurements in support of gravity science during the orbit phases of the mission. The LGAs have been designed to have broad patterns to support both safe mode telecommunications and two-way Doppler measurements for gravity science.

3 Precision Orbit Determination and Gravity Field Modeling Methodology

3.1 Precision Orbit Determination

Determination of precise orbits of the Psyche spacecraft about the asteroid requires full integration of the spacecraft trajectory from an initial state, accompanied by the application of informed models to account for non-conservative forces. Models include an *a priori* for Psyche based on astronomical estimations of GM (see Table 1), rotation parameters for Psyche (see Table 2), an initial ephemeris obtained from the JPL Solar System Dynamics group, and various other *a priori* physical parameters. In terms of published GM values, the team considers the study of Baer et al. (2011) to be most reliable because: it has the smallest uncertainty, and checking predictions for Vesta and Ceres by these authors (Baer et al. 2008) showed robust estimations. In addition we note that Baer et al. (2011) was the best value available at the time orbit design simulations were being performed (2018 time frame). Other values are listed in Table 1 to provide a compendium of published estimations.

DSN Doppler and range measurements, and optical positions acquired from the approach and Psyche mission orbital phases are co-processed to yield solutions for the spacecraft orbit, gravitational field, pole orientation and rotation rate, and heliocentric orbit. These observables are processed and filtered using JPLs MONTE (Mission Analysis, Operations, and Navigation Toolkit Environment) MONTE, which employs a least-squares approach to converge orbital arcs (Evans et al. 2018). MONTE, which has been utilized in a similar capacity in numerous other planetary gravity investigations, is capable of processing Doppler, range, and landmark observations. Processing of surface landmarks via optical imaging is accomplished using a stereophotoclinometric (SPC) process (Owen et al. 2001; Konopliv et al. 2002; Park et al. 2019, 2020).

Table 2 Psyche Physical Parameters

Parameter	Value
Spin-pole Ecliptic Longitude (λ) (deg)	35 ± 5 (Kaasalainen et al. 2002)
	32 ± 5 (Hanus et al. 2013)
	34 ± 5 (Shepard et al. 2017)
	32 ± 3 (Drummond et al. 2018)
	36 ± 2 (Shepard et al. 2021)
Spin-pole Ecliptic Longitude (β) (deg)	9 ± 5 (Kaasalainen et al. 2002)
	7 ±5 (Hanus et al. 2013)
	7 ±5 (Shepard et al. 2017)
	8 ± 3 (Drummond et al. 2018)
	8 ± 2 (Shepard et al. 2021)
Spin period (hour)	4.195947 ± 0.000001 (Kaasalainen et al. 2002)
	4.195948 ± 0.000001 (Hanus et al. 2013)
	4.195948 ± 0.000001 (Shepard et al. 2017)
	4.195948 ± 0.000001 (Drummond et al. 2018)
	4.195948 ± 0.000001 (Shepard et al. 2021)
Obliquity (deg)	94. (Bills and Scott 2021)
Maximum Dimensions (km)	279×232×189 (Shepard et al. 2021)

3.2 Data Calibration

Calibration of the tracking data is accomplished by routinely analyzing the noise level, range biases, and media effects of the Doppler and range data. Attention is focused on assuring that the quality of tracking data is at the level required to meet measurement requirements.

3.3 Gravitational Field Estimation

The gravitational field potential, $U(r, \lambda, \theta)$, associated with (16) Psyche is expressed as a spherical harmonic expansion (Kaula 1966; Heiskanen and Moritz 1967)

$$U(r, \lambda, \theta) = \frac{GM}{r}\left[1 + \sum_{l=2}^{\infty}\left(\frac{R}{r}\right)^{l}\sum_{m=0}^{l}\left(\underline{C}_{lm}\cos(m\lambda) + \underline{S}_{lm}\sin(m\lambda)\right)\underline{P}_{lm}\sin(\theta)\right] \quad (1)$$

where GM is the mass parameter, l is the spherical harmonic degree, m is the angular order, $\underline{P}_{lm}$ are the fully normalized associated Legendre polynomials, $\underline{C}_{lm}$ and $\underline{S}_{lm}$ are the normalized spherical harmonic coefficients (*cf.* Wieczorek 2015), R is the reference radius of Psyche (113 km), λ is longitude, θ is latitude, and r is the radius at the evaluation point of the Psyche spacecraft relative to the (16) Psyche body-fixed frame. Following Kaula (1966) and Lambeck (1990), the normalization of the gravity coefficients is defined such that the integral of the harmonic squared is equated to the area of a unit sphere. Normalized coefficients are related to unnormalized coefficients by

$$(C_{lm}, S_{lm}) = \left[\frac{(l-m)!(2l+1)(2-\delta_{0m})}{(l+m)!}\right]^{1/2}(\underline{C}_{lm}, \underline{S}_{lm}) \quad (2)$$

where δ is the Kronecker delta. In this formulation zonal coefficients are defined as $\underline{J}_l = -\underline{C}_{l0}$. Because the origin of the planetary system is defined to be (16) Psyche's center of mass, the degree-one coefficients are identically zero.

In practice, the potential in Eq. (1) is obtained from the inversion of normal equations in a sparse matrix of tracking observations that are weighted according to quality and spatial and temporal distribution (Balmino et al. 1982; Smith et al. 1993). A single solution yields the potential field as well as estimates of dynamical parameters that include the asteroid pole position (obliquity) and rotation rate.

4 Science Investigation

4.1 Pre-Mission Reference Field and Gravity from Shape

In order to design the Psyche mission mapping scenario and to plan for data acquisition, it is necessary to develop a reference gravity field of Psyche. Consistent with X-band tracking, the simulations assume a Doppler accuracy of 0.1 mm s $^{-1}$ and 60-s sample time. As detailed in Sect. 3.3, we develop a notional spherical harmonic expansion of the gravitational potential, defined by a reference radius, R, mass, M, and normalized spherical harmonic coefficients $\underline{C}_{lm}$ and $\underline{S}_{lm}$ (Kaula 1966; Heiskanen and Moritz 1967).

The reference gravity of (16) Psyche was computed by scaling the harmonic coefficients using the Kaula rule (Kaula 1966), an empirical power law for estimating gravitational power on solid planetary bodies. All terrestrial bodies that have measured gravitational field follow such a relationship in their degree variance spectrum (Kaula 1966; Konopliv et al. 2011; Zuber et al. 2013)

$$\sigma_l^2 = \frac{\sum_{m=0}^{l} \underline{C}_{lm}^2 + \underline{S}_{lm}^2}{(2l+1)} \tag{3}$$

Assuming a Kaula rule of $0.05\, n^{-2}$, the variance spectrum is shown in Fig. 5.

We also computed a gravity model associated with the 3-dimensional Psyche shape models from Shepard et al. (2017), which is the baseline model being used by the Psyche project. Additional shape models are also being investigated (Hanus et al. 2017; Viikinkoski et al. 2018) and the mission plan is robust with these additional models as well. The spherical harmonics of the shape model were computed using a quadrature method (Werner and Scheeres 1997) assuming the GM of 1.53 km ^{3} s^{-2}, where $G = 6.674 \times 10^{-11}$ m^3 kg^{-1} s^{-2}. The power spectrum of the baseline gravity field from the Shepard shape is shown in Fig. 5, as well as the expected accuracy of the recovered Psyche gravity field (*i.e.*, error spectrum) from Orbit C. The result shows that a $l = 10$ gravity field should be easily achievable (i.e., the intersection of the power spectrum and the error spectrum shows the recoverable resolution of the gravity field). The result also indicates that the spin pole direction can be recovered with accuracy better than 0.001° while the current estimate of Psyche's spin rate is sufficiently accurate (Shepard et al. 2021).

4.2 Implications for Psyche's Structure, Origin, Evolution and Current State

Psyche's gravity investigation is designed to yield a spherical harmonic representation of the field to better than degree and order 10 (spatial block size, or half-wavelength, average resolution of ~36 km; since Psyche is ellipsoidal the range of resolved block sizes from 30

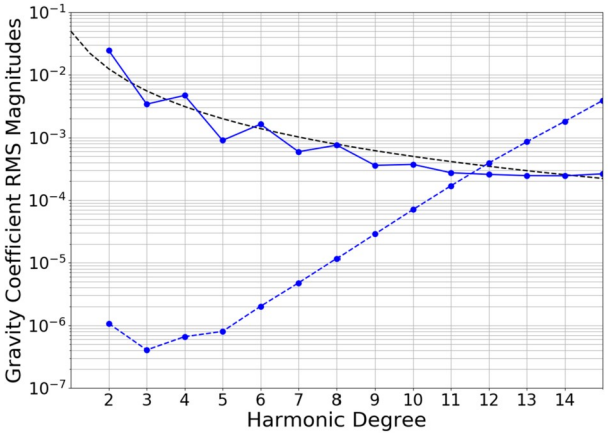

Fig. 5 Gravitational power spectra for an assumed Kaula rule (black-dashed) and for the Shepard et al. (2021) Psyche shape model (blue solid; cf. Fig. 2) assuming a constant density interior. The reference radius of Psyche was assumed to be 113 km. The power spectrum of the expected accuracy of the recovered gravity field from Orbit C is shown in the dashed-blue line. Expected accuracy is defined by the degree at which the formal error spectrum intersects the power spectrum

to 44 km), using data from Orbits A-C. This measurement depends upon the spacecraft and uplink transponder stability, and downlink signal-to-noise ratio. Each of these requirements is met with a substantial margin in performance. If we consider Orbit D in addition to Orbits A-C, we expect a degree and order 12 could be recovered (i.e., spatial resolution of ~30 km). A spherical harmonic model of free-air anomalies, derived from the differentiating the gravitational potential (Eq. (1)), will be converted to Bouguer gravity by subtracting the gravitational attraction of topography. Bouguer gravity provides information on the internal distribution of mass.

First, the Gravity Science investigation will produce a much improved estimate of the asteroid mass (cf. Table 1), reducing the uncertainty in GM to better than 0.001 km^3 s^{-2}. That measurement, combined with the volume provided from the shape determination (Jaumann et al. 2022), will provide a greatly improved estimation of bulk density. A summary of bulk density measurements of Psyche based on recent measurements of GM and volume are summarized by Elkins-Tanton et al. (2020), who notes that the bulk density is one of the highest of the main belt asteroids. The range of measured values falls in the range for other asteroids that display metal-rich surface spectra (X- and M-class; Hanus et al. 2017). The preferred current Psyche value of 3780 ± 340 kg m^{-3} (Elkins-Tanton et al. 2020) is inconsistent with Psyche being a solid metallic core. Indeed, if Psyche is metallic the bulk density implies a porosity of ~50%, a void structure that would be difficult to maintain if developed in its earliest evolution given Psyche's size and estimated early cooling rate (Nichols-Fleming et al. 2022).

Higher-degree harmonics of gravity and shape will be analyzed to discern mass variations in spatial location and depth. The gravitational flattening, $C_{2,0}$, combined with any observed spin axis precession, if it occurs and is measurable, will permit estimation of C/MR^2, the moment of inertia factor that provides a measure of the radial distribution of mass. If Psyche's structure predominantly reflects solidification from a liquid, it should exhibit radial variation in its density structure and approximate azimuthal symmetry after accounting for effects of impacts, which will have greatest effect at shallow depths. As a case in point, a model of Vesta's gravity field with an assumed three-layer model showed nearly perfect correlation for all measurable degrees (Konopliv et al. 2014; Park et al. 2014), indicating no substantial density variations in the thickness or density of Vesta's crust. Azimuthal symmetry, at least at crustal levels, can also be achieved by impact homogenization, as has been observed for the Moon (Zuber et al. 2013). Estimates of the effective surface density

for each spherical harmonic degree will provide constraints on how the density varies with depth (Wieczorek 2013; Besserer et al. 2014). Gravity, like all potential field data, provides non-unique interpretations. In particular, internal mass variations can be associated with either compositional variations or porosity. The addition of other data allows the range of interpretations to be narrowed.

If Psyche was instead substantially disrupted and/or was never molten, it will likely have a more heterogeneous density structure. Correlation of its gravity field with surface topography (Jaumann et al. 2022) via transfer function techniques of admittance and coherence, would indicate spatial regions where the density structure is not consistent with simple azimuthally symmetric models. Gravity and shape combined with magnetometry (Weiss et al. 2022) and surface compositional data (Bell et al. 2022; Lawrence et al. 2022), will be collectively required to constrain the structure and degree of azimuthal symmetry, including the possible disruption of the body into a rubble pile (Elkins-Tanton et al. 2022). If Psyche does turn out to be largely metallic, it almost certainly will have acquired its porosity subsequent to cooling.

The spatial resolution of gravity noted above, combined with that of topography (50 m pixel^{-1}; Jaumann et al. 2022) dictates that regional density variations across Psyche's shallow subsurface, including in association with large craters (Marchi et al. 2022) can be mapped. And combined with surface observations to provide geophysical information to support geological context based on observations from other Psyche sensors (Jaumann et al. 2022; Lawrence et al. 2022; Marchi et al. 2022).

5 Data Archiving and Distribution

Standard data products from the Psyche Gravity Investigation will be archived in the Small Bodies Node of the NASA Planetary Data System on a schedule set by the Psyche Project, as per its contract with NASA. Level 0 data products, in TRK-34 format, will be delivered to the PDS for verification and archiving within 6 months of collection and will be disseminated to the scientific community immediately upon verification by PDS reviewers.

Level 3 data, including spherical harmonic models of gravitational potential, free air gravity and Bouguer gravity, and determinations of other physical parameters (*e.g.*, planetocentric reference frame, spin-pole axis, rotation rate, etc.) will be archived at a Planetary Data System (PDS) Small Bodies Node as part of the Psyche archival plan.

6 Summary

The Psyche mission affords the unprecedented opportunity to map a possible protoplanetary core. Gravity observations, combined with other orbital observations of topography, magnetometry and compositional measurements, will collectively provide a quantitative view of the internal mass distribution and implications for origin and composition.

Acknowledgements This investigation is supported by the NASA Psyche Mission. A portion of this research was carried out at the Jet Propulsion Laboratory, California Institute of Technology, under a contract with the National Aeronautics and Space Administration (80NM0018D0004).

References

S.W. Asmar et al., Spacecraft Doppler tracking: noise budget and accuracy achievable in precision radio science observations. Radio Sci. **40** (2005). https://doi.org/10.1029/2004RS003101

J. Baer et al., An observational error model, and application to asteroid mass determination. Bull. Am. Astron. Soc. **40**, 493 (2008)

J. Baer et al., Astrometric masses of 26 asteroids and observations on asteroid porosity. Astron. J. **141**, 1–12 (2011)

J. Baer, S.R. Chelsey, Simultaneous mass determination for gravitationally coupled asteroids. Astron. J. **154**, 76 (2017). https://doi.org/10.3847/1538-3881/AA7DE8

G. Balmino et al., Gravity field of Mars in spherical harmonics up to degree and order eighteen. J. Geophys. Res. **87**, 9735–9746 (1982)

J.F. Bell et al., The multispectral imaging investigation on the NASA Psyche discovery mission. Space Sci. Rev. (2022, this journal). https://doi.org/10.1007/s11214-022-00874-7

J. Besserer et al., GRAIL gravity constraints on the vertical and lateral density structure of the lunar crust. Geophys. Res. Lett. **41**, 5771–5777 (2014). https://doi.org/10.1002/2014GL060240

B. Bills, B.R. Scott (2021). https://ui.adsabs.harvard.edu/abs/2019AGUFM.P51E3412B/abstract

M. Brown et al., Psyche spacecraft design. Space Sci. Rev. (2021, this journal). https://doi.org/10.1109/AERO.2018.8396444

B. Carry et al., Density of asteroids. Planet. Space Sci. **73**, 98–118 (2012)

J.D. Drummond et al., The triaxial ellipsoid size, density, and rotational pole of asteroid (16) Psyche from Keck and Gemini AO observations 2004–2015. Icarus **305**, 174–185 (2018). https://doi.org/10.1016/j.icarus.2018.01.010

L.T. Elkins-Tanton, The taxonomy of planetesimals: consequences for planets, in *Planetesimals: Early Differentiation and Consequences for Planets*, ed. by L.T. Elkins-Tanton, B.P. Weiss (Cambridge University Press, Cambridge, 2016), pp. 365–375

L.T. Elkins-Tanton et al., Observations, meteorites, and models: a preflight assessment of the composition and formation of (16) Psyche. J. Geophys. Res., Planets **125**, e2019JE006296 (2020). https://doi.org/10.1029/2019/JE006296

L.T. Elkins-Tanton et al., Distinguishing the origin of (16) Psyche. Space Sci. Rev. (2022, this journal). https://doi.org/10.1007/s11214-022-00880-9

S. Evans et al., MONTE: the next generation of mission design and navigation software. CEAS Space J. **10**, 79–86 (2018). https://doi.org/10.1007/s12567-017-0171-7

J. Hanus et al., Sizes of main-belt asteroids by combining shape models and Keck adaptive optics observations. Icarus **226**, 1045–1057 (2013). https://doi.org/10.1016/j.icarus.2013.07.023

J. Hanus et al., Volumes and bulk densities of forty asteroids from ADAM shape modeling. Astron. Astrophys. **601**, A114 (2017). https://doi.org/10.1051/0004-6361/201629956

W. Hart et al., Overview of the spacecraft design for the Psyche mission concept, in *IEEE Aerospace Conf.*, Big Sky, MT (2018), pp. 1–20

W.A. Heiskanen, H. Moritz, *Physical Geodesy* (W.H. Freeman, San Francisco, 1967), 404 pp.

R. Jaumann et al., The Psyche topography and geomorphology investigation. Space Sci. Rev. (2022, this journal). https://doi.org/10.1007/s11214-022-00874-7

M. Kaasalainen et al., Models of twenty asteroids from photometric data. Icarus **159**, 369–395 (2002). https://doi.org/10.1006/icar.2002.6907

W.M. Kaula, in *Theory of Satellite Geodesy*, Waltham, Blaisdell (1966), 124 pp.

O.M. Kochetova et al., Determination of large asteroid masses by the dynamical method. Sol. Syst. Res. **38**, 66–75 (2004)

A.S. Konopliv et al., A global solution for the gravity field, rotation, landmarks, and ephemeris of Eros. Icarus **166**, 289–299 (2002)

A.S. Konopliv et al., The dawn gravity investigation at Vesta and Ceres. Space Sci. Rev. **163**, 461–486 (2011). https://doi.org/10.1007/s11214-011-9794-8 Also in *The Dawn Mission to Minor Planets 4 Vesta and 1 Ceres*, ed. by C.T. Russell, C.A. Raymond
A.S. Konopliv et al., The Vesta gravity field, spin pole and rotation period, landmark positions, and ephemeris from the Dawn tracking and optical data. Icarus **240**, 103–117 (2014). https://doi.org/10.1016/j.icarus.2013.09.005
A.S. Konopliv et al., A global solution for the gravity field, rotation, landmarks, and ephemeris of Eros. Icarus **299**, 411–429 (2018). https://doi.org/10.1016/j.icarus.2017.08.005
M. Kuzmanoski, A. Kovačević, Motion of the asteroid (13206) 1997GC22 and the mass of (16) Psyche. Astron. Astrophys. **395**, L17–L19 (2002)
P. Kuchynka, W.M. Folkner, A new approach to determining asteroid masses from planetary range measurements. Icarus **222**, 243–253 (2013).
K. Lambeck, *Geophysical Geodesy* (Cambridge University Press, New York, 1990)
D.J. Lawrence et al., The Psyche gamma ray % neutron spectrometer investigation. Space Sci. Rev. (2022, this journal)
S. Marchi et al., Determining the relative cratering ages of regions of Psyche's surface. Space Sci. Rev. (2022, this journal). https://doi.org/10.1007/s11214-022-00891-6
F. Nichols-Fleming et al., Porosity evolution in metallic asteroids: implications for the origin and thermal history of asteroid 16 Psyche. J. Geophys. Res., Planets **127**, e2021JE007063 (2022). https://doi.org/10.1029/2021JE007063
D.Y. Oh et al., Development of the Psyche mission for NASA's discovery program, in *The 36th Electric Propulsion Conf., IEPC-2019-192*, 12-20 September 2019 (Univ. Vienna, Austria, 2019), 29 pp.
W.M. Owen Jr. et al., in *NEAR Optical Navigation at Eros. AAS/AIAA Astrodynamics Specialists Conference*, Quebec City, Quebec, CA (2001)
R.S. Park et al., Gravity field expansion in ellipsoidal harmonic and polyhedral internal representations applied to Vesta. Icarus **240**, 118–132 (2014). https://doi.org/10.1016/j.icarus.2018.10.024
R.S. Park et al., A partially differentiated interior for (1) Ceres deduced from its gravity field and shape. Nature **537**, 515–517 (2016). https://doi.org/10.1038/nature18955
R.S. Park et al., High-resolution shape model of Ceres from stereophotoclinometry using Dawn imaging data. Icarus **319**, 812–827 (2019). https://doi.org/10.1016/j.icarus.2018.10.024
R.S. Park et al., Evidence of non-uniform crust of Ceres from Dawn's high-resolution gravity data. Nat. Astron. **4**, 748–755 (2020). https://doi.org/10.1038/s41550-020-1019-1
C.A. Polanskey et al., Psyche science operations concept: maximize reuse to minimize risk, in *SpaceOps Conf.*, Marseille, France (2018)
C.T. Russell et al., Dawn mission to Vesta and Ceres: symbiosis between terrestrial observations and robotic exploration. Earth Moon Planets **101**, 65–91 (2007). https://doi.org/10.1007/s11038-007-9151-9
M.K. Shepard et al., Radar observations and shape model of asteroid 16 Psyche. Icarus **281**, 388–403 (2017). https://doi.org/10.1018/j.icarus.2014.09.016
M.K. Shepard et al., Asteroid 16 Psyche: shape, features, and global map. Planet. Sci. J. **2**, 125 (2021). https://doi.org/10.3847/PSJ/abfdba
L. Siltala, M. Granvik, Mass and density of asteroid (16) Psyche. Astrophys. J. Lett. **909**, L14 (2021). https://doi.org/10.3847/2041-8213/abe948
D.E. Smith et al., An improved gravity model for Mars: Goddard Mars Model-1 (GMM-1). J. Geophys. Res. **98**, 20871–20889 (1993)
L. Somenzi et al., etermination of asteroid masses from their close encounters with Mars. Planet. Space Sci. **58**, 858–863 (2010)
M. Viikinkoski et al., (16) Psyche: a mesosiderite-like asteroid. Astron. Astrophys. **619**, L3 (2018) (1993). https://doi.org/10.1051/0004-6361/201834091
B. Viateau et al., Mass and density of asteroids (16) Psyche and (121) Hermione. Astron. Astrophys. **354**, 725–731 (2000)
B.P. Weiss et al., The Psyche magnetometry investigation. Space Sci. Rev. (2022, this journal)
R.A. Werner, D.J. Scheeres, Exterior gravitation of a polyhedron derived and compared with spherical harmonic and mascon gravitation representations of asteroid 4769 Castalia. Celest. Mech. Dyn. Astron. **65**, 313–344 (1997)
M.A. Wieczorek, The crust of the Moon as seen by GRAIL. Science **339**, 671–675 (2013). https://doi.org/10.1126/science.1231530
M.A. Wieczorek, *Gravity and Topography of the Terrestrial Planets, Treatise on Geophysics*, 2nd edn. (Elsevier, Oxford, 2015), pp. 153–193. https://doi.org/10.1016/B978-0-444-53802-4.00169-X
M.T. Zuber et al., Gravity field of the Moon from the Gravity Recovery and Interior Laboratory (GRAIL) mission. Science **339**, 668–671 (2013). https://doi.org/10.1126/science.1231507